

Enhancing Efficiency in Multidevice Federated Learning through Data Selection

Fan Mo*
Imperial College London, UK

Mohammad Malekzadeh
Nokia Bell Labs, UK

Soumyajit Chatterjee
Nokia Bell Labs, UK

Fahim Kawsar
Nokia Bell Labs and University of Glasgow, UK

Akhil Mathur
Nokia Bell Labs, UK

Abstract

Ubiquitous wearable and mobile devices provide access to a diverse set of data. However, the mobility demand for our devices naturally imposes constraints on their computational and communication capabilities. A solution is to locally learn knowledge from data captured by ubiquitous devices, rather than to store and transmit the data in its original form. In this paper, we develop a federated learning framework, called Centaur, to incorporate *on-device data selection* at the edge, which allows *partition-based training* of a deep neural nets through collaboration between constrained and resourceful devices within the *multidevice ecosystem of the same user*. We benchmark on five neural net architecture and six datasets that include image data and wearable sensor time series. On average, Centaur achieves $\sim 19\%$ higher *classification accuracy* and $\sim 58\%$ lower *federated training latency*, compared to the baseline. We also evaluate Centaur when dealing with imbalanced non-iid data, client participation heterogeneity, and different mobility patterns. To encourage further research in this area, we release our code at github.com/nokia-bell-labs/data-centric-federated-learning.

CCS Concepts

• Computing methodologies → Distributed computing methodologies; Machine learning; • Human-centered computing → Ubiquitous and mobile computing.

Keywords

Federated Learning, Constrained Devices, Data Selection, Partition-Based Training, Edge Intelligence, On-device AI

1 Introduction

With the growing trend of utilizing ubiquitous devices in personal and industrial environments, federated learning (FL) enables the discovery of new patterns in personal data by training deep neural networks (DNNs) on data captured by various users in a more private manner [24, 40]. Especially, in a multidevice ecosystem, the owner can seamlessly share data across the devices within their trusted environment

*Work done at Nokia Bell Labs, Cambridge, UK

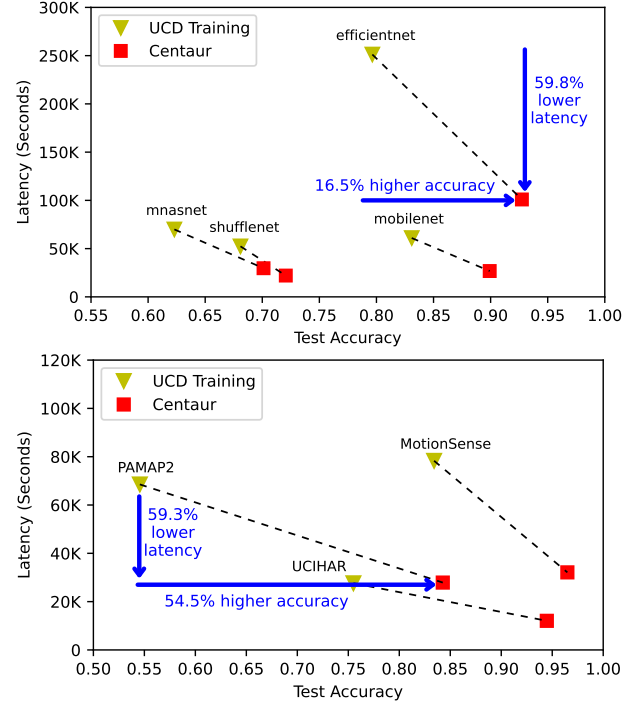


Figure 1: The latency of federated training versus classification accuracy on test dataset. We compare Centaur with standard federated training that only trains the classifier on ubiquitous constrained devices (UCDs) without data selection and partition-based training. (Top plot) Four models were tested on image data from CIFAR-10, and (bottom plot) a model was tested on three datasets of wearable sensor time-series.

while protecting data privacy [10]. This allows us to utilize the capabilities of multiple devices to participate in the FL process. However, wearable and ubiquitous devices have limited computing resources, little on-device storage, and inconsistent network connectivity.

Most of the existing FL frameworks do not account for constraints of personal devices and instead assume either modern smartphones [20, 43], or edge devices with DNN

accelerators [10, 59], as target client devices. Although smartphones and accelerators are less powerful than cloud machines, they are nevertheless equipped with mobile GPUs, possess gigabytes of runtime memory, and have fairly stable connectivity to a central server, which simplifies the requirements of DNN training [34, 56].

In this paper, we propose a novel FL framework to include *ubiquitous constrained devices* (UCDs), *i.e.*, wearable devices such as earbuds, glasses, or rings, or distributed edge devices such as environmental cameras or industrial sensors. We believe UCDs are becoming the primary *data-producing* devices for both individuals and industries, due to various on-device sensors, such as cameras or inertial measurement units. These devices offer a wealth of spatiotemporal data that is frequently absent when focusing solely on smartphones or plugged-in devices. For example, people often opt for wristbands, smart rings, or earbuds over carrying a smartphone in their hand or pocket while engaging in outdoor, industrial, or sports activities [42, 47], and sensors distributed across farms or forests remotely monitor crops and livestock to detect hazards [44]. The main *motivation* of our work is the fact that the abundance and diversity in data captured by ubiquitous devices can facilitate learning more effective models for emerging applications in personal and industrial environments.

There are several significant *challenges*. Usually, distributed or wearable UCDs use an *access point* (AP), like a smartphone or a router, as a relay to connect to a *central server* in the cloud. Data captured by a UCD is communicated to the AP using communication protocols like Bluetooth Low Energy (BLE). In outdoor settings under mobility, UCDs may not always be connected to the companion AP, thus inaccessible to the central server. Beside this, the constrained data storage and computing resources will restrict the size and functionality of DNNs that can be trained locally on UCDs. A naive solution is to transfer all data from UCDs to their respective APs and perform training of DNNs on APs. Yet, storing *all* data could exceed the device’s memory, especially when UCDs disconnect from their AP. To demonstrate these points, in §3, we conduct a motivating study on a real testbed to identify the essential design requirements that can enable the deployment of FL on resource-constrained devices. To tackle these challenges effectively, we believe FL solutions relying on on-device training should dynamically distribute data and computations between UCDs and their companion APs.

In §4 and Figure 3, we introduce **Centaur**: a federated learning framework that orchestrates local training among UCDs and APs by integrating **on-device data selection** with **partition-based model training**.

(A) Considering computation constraints, we initialize the DNN in two partitions: an *encoder* (*i.e.*, feature extractor) to be only trained on APs, followed by a lightweight *classifier* to

be trained on both APs and UCDs (§4.1). This allows Centaur to utilize all the data available on UCDs for fine-tuning the DNN while occasionally storing and transmitting a portion of the data to the APs to re-train the entire DNN and adjust to the runtime variability in data distributions [19, 50, 53].

(B) Considering memory and connectivity constraints, we perform data selection [23] by analyzing the *training loss* and the *gradients norm* of the classifier part, to decide which data points captured by UCDs contribute more to the training of which part of the DNN. Through data selection, data points are categorized as either of (i) *discarded* if they have very low loss values, (ii) *kept* locally on the UCD to train the classifier part if their loss values or gradients norm are not very high, and (iii) *transmitted* to the AP to train both encoder and classifier part if they cause high values for both loss and gradients norm (§4.2). We assume that each pair of UCD and AP belongs to the same client, thus transmitting data from a UCD to its AP does not violate the clients’ privacy.

(C) We benchmark on five DNNs architectures and six datasets of two different modalities, and compared to existing FL alternatives. Our results show that Centaur saves more *bandwidth* by reducing the communication cost associated with offloading samples from a UCD to the AP, and also reduces the *latency* of training (and accordingly the *energy* consumption) on both UCD and AP. As a prime example of our experimental results, Figure 1 shows the training latency versus classification accuracy of performing FL for two different tasks: (1) four benchmark DNNs, with their encoder pre-trained on ImageNet [14], and then trained for CIFAR10 [28] image classification with 100 FL clients, and (2) a benchmark ConvNet [9], trained from scratch, on three human-activity recognition datasets with 20 FL clients. In both figures, we compare Centaur with the baseline of standard FL on UCDs without our implemented strategies. Centaur, through data selection and partition-based model training, achieves up to 19% higher accuracy and 58% lower latency, on average.

The **key contribution** of our work is a better integration of ubiquitous constrained devices into federated learning by leveraging the advantages of multi-device ecosystems. We achieve this by introducing a customizable data selection scheme and a partition-based training approach, which collectively reduce computational and communication costs while enhancing model accuracy. Our experiments demonstrate that Centaur effectively minimizes storage requirements and training time through efficient data selection. Furthermore, our analysis accounts for the real-world spatiotemporal mobility of edge devices in FL. Empirical evaluations, covering cost, data imbalance, participation heterogeneity, and connection probability, show that Centaur consistently delivers higher efficiency, achieving improved accuracy at lower costs across diverse scenarios.

Table 1: Related work. (1) *Model Partitioning* splits the model into an encoder and a classifier. (2) *Data Selection* trains on a subset of available data. (3) *On-device Training* on constrained devices. (4) *Spatiotemporal Coverage* includes portable devices.

	Model Partitioning	Data Selection	On-device Training	Spatiotemporal Coverage
Multitier FL [1, 2, 10, 19, 35]	×	×	×	×
Split FL [7, 12, 15, 31, 57, 58]	✓	×	×	×
On-device Training [4, 18, 22, 27, 30, 32, 33, 55]	×	×	✓	✓
Centaur (ours)	✓	✓	✓	✓

2 Related Work

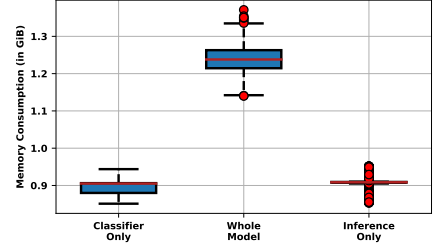
Table 1 compares Centaur with major prior work on different aspects of multidevice FL. Compared to the standard edge-server FL, edge-access point-server FL [1, 35] considers a middle layer, *e.g.*, a cellular base station, to orchestrate FL training across clients and a central server. Clients can participate with several devices [10, 15, 58], which achieve better trade-offs between accuracy and bandwidth consumption. However, these works assume the local training of the entire model on edge devices, without any resource limitations. They also do not utilize the potential of resource-rich devices to assist a resource-constrained device during training. They use APs only for aggregation and communication, which makes FL impractical in scenarios involving UCDs.

Other works consider inference only (*i.e.*, forward pass) [4, 18, 32, 55], sparse training [7, 31], or heterogenous architectures across clients of different capabilities [25, 45]. Sparse training or pruning requires computational resources (especially memory) that UCDs do not have. Few works propose solutions for full on-device training (*i.e.*, forward and backward pass) [33], but not for FL scenarios as they often make impractical assumptions like the availability of large datasets for network architecture search [32], or unconstrained memory for training the full model [15, 58]. Transfer learning can be used on UCDs to fix the encoder architecture, which in turn restricts the extraction of newer features, and only trains the last layer for the personalized training [58].

Without utilizing the power of APs, training the entire model on UCDs requires a large sample size to learn generalized features [7, 31]. Simply considering different sub-models [15, 25, 45] requires more sophisticated aggregation strategies and shallower models for resource-constrained devices, which may not be capable of learning the complex patterns from the data. Recent works enable training on micro-controllers with limited memory, such as TensorFlow Lite Micro [13] or Tiny Training Engine [33]. These works do not consider FL as a potential use case and do not account for the advantages of a multidevice ecosystem.



(a) The Testbed



(b) Memory Consumption

Figure 2: Running FL on four RaspberryPi, we measure memory for when (i) only the classifier is trained, (ii) the entire model is trained, and (iii) the entire model runs inference only.

3 A Motivating Study

As depicted in Figure 3, a *ubiquitous constrained device* (UCD) is a portable device with restricted hardware and connectivity resources. An *access point* (AP) is a resourceful device that has much better hardware and connectivity capabilities than its corresponding UCD. We assume the AP is always part of the user’s device ecosystem that allows the UCD to transmit data to the AP without violating the user’s privacy. A *server* is a central entity owned by a service provider that orchestrates FL over several clients. Considering a deep neural network architecture, an *encoder* (E) is the first part of the DNN that extracts the features from input data. A *classifier* (C) is the second part of the DNN, which performs the final classification using the encoded features. We consider supervised learning tasks where X denote the input data and y denote its label.

Setup. To identify the key design choices, we create a testbed with four RaspberryPi 4 Model B as edge devices [16, 51]; all running the 64-bit Raspbian OS with total secondary storage of 32GB. We set up four clients with varying primary memories: C1, C2, C3, and C4 having 1GB, 2GB, 4GB, and 2GB, respectively. For analyzing the CPU and memory consumption of the clients, we use logs of `/proc/stat` and free operating-system calls, respectively. We use MobileNetV3 [21], pre-trained on ImageNet, as the encoder followed by two fully-connected layers with an intermediate drop-out layer. Using CIFAR10, we measure the resources and time needed for both on-device training (per epoch) and inference. We implement FL with Flower [5] and use a desktop computer as the server, as shown in Figure 2a.

Key Observations. We run FedAvg [40] for 100 rounds with four RaspberryPi devices, considering two scenarios: (1) when only the classifier part is trained, and (2) when the entire model (encoder and classifier) is trained. When running our experiments for the first scenario, we observed

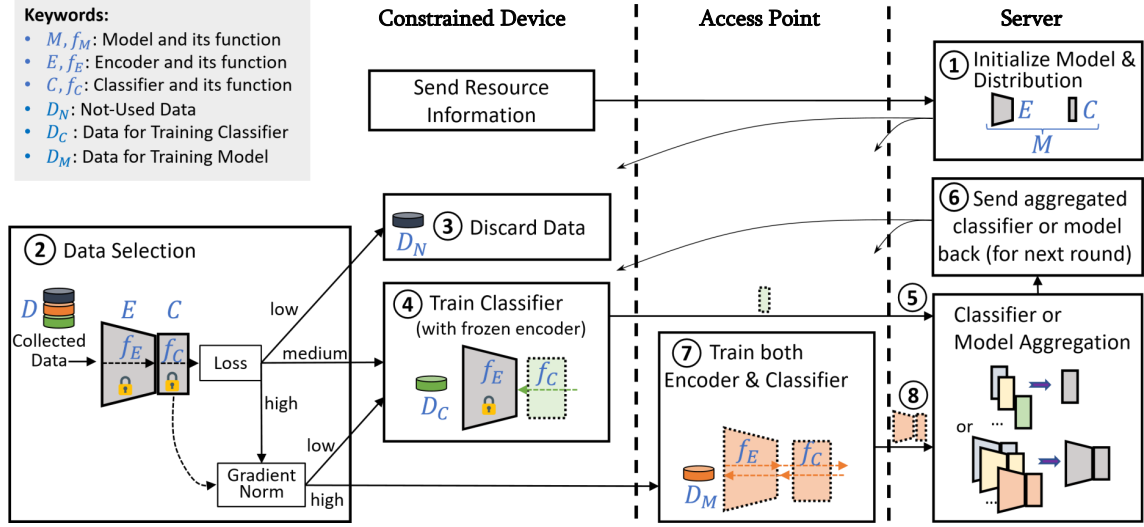


Figure 3: The overview of Centaur, including model initialization (§ 4.1), data selection (§ 4.2), and partition-based training and aggregation (§ 4.3). We explain the set up in § 4 and elaborate the details of Steps ① to ⑧.

that the standard FL runs successfully over all four clients. However, for the second scenario, client C1 with 1GB of primary memory always failed to participate in the FL process. This is primarily due to the significant rise in the CPU and memory consumption when the entire model (both encoder and classifier) are trained on the device (see Figure 2).

Notably, 1GB of primary memory is still significant in terms of memory capability, and many UCDs may have significantly less memory than this. Therefore, it is clear that in such cases, it is much more challenging to deploy standard FL over UCDs. Moreover, training only the classifier consumes far less resources and is even comparable to the resource usage required for a forward pass. We noticed a similar pattern for time consumption, where training the classifier only is 50× time efficient compared to training the entire model. One alternative solution to decrease the overall training time is to reduce the training data size by randomly discarding samples. However, we observe that such an approach comes at a cost of significantly reduced accuracy, which is detrimental to the overall system.

4 Method

In Figure 3, we introduce Centaur, our federated learning framework. Here, we elaborate on each component in detail.

Step ①: The server receives the information about UCDs’ resource. Accordingly, the server initializes a DNN model M that is formed of an encoder E and a classifier C , and then distributes the E and C to the APs and subsequently to UCDs. We explain model initialization details in §4.1.

Step ②: UCDs start FL by performing data selection on the collected data D , based on the computed loss value via

the forward pass and the magnitude of the gradient of the classifier’s last layer. Each sample point will be categorized in one of (i) D_N to be discarded, (ii) D_C for locally training C on the UCD, or (iii) D_M to be transmitted to AP for training M . We explain data selection details in §4.2.

Step ③: The UCD discards data D_N in the current epoch without any further training steps or backward pass on them.

Step ④: The UCD performs backward pass through the classifier C on data D_C , while the encoder E is frozen. Then, the UCD updates the parameters of C via computed gradients. Notice that, in practice, the gradient computation done in Step ② can be reused for this update.

Step ⑤: UCDs share their updated classifier C to the server, and the server performs aggregation on all C from participating UCDs to obtain one aggregated classifier.

Step ⑥: The server sends the aggregated classifier back to the UCDs and APs.

Step ⑦: With the updated classifier, the AP trains the encoder E together with the classifier C atop E on data D_M . That is, D_M is fed for a forward pass and then a backward pass throughout to update M .

Step ⑧: The updated M (including E and C) is shared from the AP to the server. After collecting updated M from all participating APs, the server performs model aggregation to obtain the aggregated encoder E and classifier C and distributes them back to UCDs and APs as in Step ⑥. See § 4.3 for more details of FL training procedures.

Steps from ② to ⑧ will be repeated for $R/2$ rounds to update C on UCDs and E on APs. Algorithm 1 shows the process of partition-based training and aggregation in Centaur.

Algorithm 1 Centaur: Multidevice Federated Learning via Partition-based Training and Data Selection

1 **Inputs:** (1) \mathcal{A} : the set of A clients each having two devices, one UCD and one AP, (2) D^k : local dataset for each client $a \in \{1, \dots, A\}$, (3) f_E : the encoder part with parameters W_E , (4) f_C : the classifier part with parameters W_C , (5) R : the total number of FL rounds.

2 **for** $r \in \{1, \dots, R/2\}$ **rounds do**

3 K clients \leftarrow randomly select K clients from a total of A , using uniform sampling

– Training on UCDs –

4 **for** $k \in \{1, \dots, K\}$ **do**

5 $\mathbf{X}^k, \mathbf{y}^k \leftarrow D^k$ (all the samples in the local dataset of client k UCD)

6 $\ell^k = \mathcal{L}(f_E \circ f_C(\mathbf{X}^k), \mathbf{y}^k)$ (forward pass to compute per-sample loss values)

7 $D_N^k, D_C^k, D_M^k \leftarrow$ based on ℓ^k , perform data selection as detailed in Section 4.2

8 **for all** $(\mathbf{X}_j^k, \mathbf{y}_j^k) \in D_C^k$ **do**

9 $g_C^k = \partial \ell^k / \partial W_C$ (compute f_C 's gradients on D_C^k to update f_C)

10 $W_C^k = \text{Optimizer}(W_C^k, g_C^k)$ (update f_C 's parameters using gradients)

11 $D^+ \leftarrow$ based on g_C^k , perform data selection as detailed in Section 4.2

12 $D_M^k = D_M^k \cup D^+$ (enhance D_M^k by high-value gradients data points)

– Server Side Aggregation on the Classifier Part –

13 $W_C \leftarrow \frac{1}{K} \sum_{k \in K} W_C^k$

14 $W_C^k \leftarrow W_C$ (update all clients with new W_C)

– Training on APs –

15 **for** $k \in \{1, \dots, K\}$ **do**

16 $\mathbf{X}^k, \mathbf{y}^k \leftarrow D_M^k$ (all selected samples for training f_E on client k AP)

17 $\ell^k = \mathcal{L}(f_E \circ f_C(\mathbf{X}^k), \mathbf{y}^k)$ (forward pass to compute per-sample loss values)

18 $g^k = \partial \ell^k / \partial (W_E, W_C)$ (compute gradients on D_M^k to update f_E and f_C)

19 $W_E^k, W_C^k = \text{Optimizer}(W_E^k, W_C^k, g^k)$ (update all parameters using gradients)

– Server Side Aggregation on both Encoder and Classifier Parts –

20 $\{W_E, W_C\} \leftarrow \frac{1}{K} \sum_{k \in K} \{W_E^k, W_C^k\}$

21 $\{W_E^k, W_C^k\} \leftarrow \{W_E, W_C\}$ (update all clients with the new aggregated model)

22 **return** $\{W_E, W_C\}$

4.1 Model Initialization

To partition a DNN into an encoder E and a classifier C , one option is to use pre-trained benchmark DNNs; considering numerous well-trained models. Usually, DNN architectures from a candidate space of pre-trained models have

already been well developed, with efficient quantization and compression capabilities, to be deployed on UCDs for inference [4, 18, 31, 32, 55]. We aim to utilize the full capability of UCDs for on-device training of the classifier C . Thus, we need to design the classifier such that it can run on the limited memory and computation power available on these devices. To achieve these, we can iteratively look into candidate architectures that fit in the limited memory available on these UCDs. A robust mechanism in this direction is to obtain a history of memory usage of a particular device, which reflects the typical memory availability on the UCD. Formally speaking, the iterative process can be viewed as an optimization problem described as

$$C = \min\{m_1, m_2, \dots, m_k | \mathbb{P}(m_k) \times \mathbb{B} < \mathbb{M}\}, \quad (1)$$

where $\mathbb{P}(m_k)$ provides the number of parameters of the candidate architecture m_k , \mathbb{B} is the number of bytes used to store the parameters and intermediate results in computations, and \mathbb{M} is the memory available in the device for FL participation. The parameter \mathbb{M} can be measured and logged as empirical observations of the UCD memory usage, to be sent to the server as we discussed in Step ① in Figure 3.

Here, we select our classifier architectures as fully connected layers. Thus, by either reducing the number of neurons or the layers, one can find a potential classifier C that can fit into the requirements for Equation (1). In the same vein, the problem of low computing resources is addressed by choosing the smallest architecture for C and then deploying it on the UCDs.

4.2 Data Selection

We determine the importance of each data sample, along the forward pass, to decide whether to further perform (the more costly) backward pass on this sample or not. Such data selection satisfies design requirements by improving both storage efficiency and training efficiency. We use a combination of (i) the *loss value* and (ii) the *norm of last-layer gradients* to measure the sample's importance.

4.2.1 Loss-based Selection. All available data D at round r are fed into the model M to compute their loss values $\ell_r(f_M(\mathbf{X}), \mathbf{y})$. We consider lower loss values as an indication of being less important, and higher loss values show the importance of the data [23]. To this end, at round r for the current ℓ_r , we drive a cumulative distribution function (CDF_r^ℓ). Then at round $r + 1$, the probability of discarding data, \mathcal{P}_N , and the probability of feeding data to train the complete model M on AP, \mathcal{P}_M , are defined as:

$$\begin{cases} \mathcal{P}_N(\ell_{r+1}) = 1 - [\text{CDF}_r^\ell(\ell_{r+1})]^\alpha \\ \mathcal{P}_M(\ell_{r+1}) = [\text{CDF}_r^\ell(\ell_{r+1})]^\beta \end{cases} \quad (2)$$

where α and β parameters determine the level of selectivity. At round $r + 1$, for a sample with loss value ℓ_{r+1} , the sample is selected into D_N with probability of $\mathcal{P}_N(\ell_{r+1})$. Thus, the lower the loss value for a sample, the greater the probability for being discarded. Similarly, \mathcal{P}_M selects samples with the highest losses as D_M ; which means that the higher the loss value for a sample, the greater the probability of being chosen to train the entire model. Samples that are not selected for D_N or D_M are added to D_C to locally train C on the UCD. We use a fixed-size queue for the CDF_r^ℓ to dynamically keep track of loss values so that the \mathcal{P}_N and \mathcal{P}_M for the current sample can be efficiently computed using its loss and to save computational resources similar to prior work [29].

4.2.2 Gradient-based Selection. For samples that are *not* selected through \mathcal{P}_N and \mathcal{P}_M , and to avoid consuming extra resources of UCDs, we can further compute the gradients of the classifier’s last layer. The norm of these gradients gives us a useful hint about the sample’s importance while requiring much less computation than computing all layers’ gradients [26]. The last layer’s norm at round r is produced during training of the classifier by $g_r = \frac{\partial \ell_r}{\partial W_r}$, where W_r is the weights of the classifier C ’s last layer at round r . Following the same idea, we derive a CDF_r^g for gradient norm values and build a queue to keep track of the computed norm of gradient values. Samples with larger gradients have larger impacts on the model’s weights; thus, we also keep these samples for training the entire model M as E might learn new “features” from them. Thus, the probability of adding a sample to D_M at round $r + 1$ is defined as:

$$\mathcal{P}_M^+(\|g_{r+1}\|) = [\text{CDF}_r^g(\|g_{r+1}\|)]^\gamma \quad (3)$$

where γ is used for customizing the selection rate. Samples with high norm are selected with $\mathcal{P}_M^+(\|g_{r+1}\|)$ and then added to data D_M . Our dynamic strategy, in combining loss and last-layer gradient norm, enables Centaur to achieve a better trade-off between computation cost and selection performance on UCDs. Moreover, one may substitute this module with a different data selection technique that could also be dependent upon the specific use case.

4.3 Partition-based Training and Aggregation

Training is conducted on both UCDs and APs. While UCDs only train the classifier C on data D_C , APs train the complete model M on data D_M . Such a procedure allows the model to be (partially) updated when UCDs are offline, in addition to the full updates when UCDs have a connection to the internet. This better utilizes UCDs’ spatiotemporal richness and consequently improves the training efficiency in our design requirements.

Algorithm 1 shows partition-based training and aggregation in Centaur, running $R/2$ rounds, considering that UCD training and AP training proceed iteratively in one round. All training is conducted on the client’s devices either on UCDs or APs. Then with all updated weights, the server performs Federated Averaging (FedAvg) [40] to obtain one aggregated global model. The new global model needs to be distributed to all clients UCDs and APs such that (i) the training on AP has an updated classifier, and (ii) the training on UCD in the next round has both an updated encoder and classifier.

5 Experimental Setup

Datasets. We use six commonly used datasets. CIFAR10 and CIFAR100 [28] that both include 50K training samples and 10K test samples, with 10 and 100 classes, respectively. EMNIST [11] that includes 112K training samples with 47 classes. UCIHAR [3] is a widely used dataset of 30 users performing 6 daily activities; data from the accelerometer and gyroscope sensors were collected by a smartphone worn on the waist. Data from 21 users is used for training, and that of the other 9 users for testing purposes. MotionSense [38] also includes accelerometer and gyroscope data from 24 users with a smartphone in the pocket of the trousers who performed 6 activities in 15 trials. We use as test data one trial session for each user and as training data the remaining trial sessions (e.g., one trial of “walking” of each user is used as test data and the other two trials are used as training). PAMAP2 [46] dataset contains data of 13 different physical activities, performed by 9 subjects wearing 3 devices and a heart rate monitor. We use the training-test split provided by the PersonalizedFL library [36].

Models. For image classification datasets, we select four DNNs commonly used in mobile/edge-oriented literature: (1) EfficientNet-v2 [49], (2) MobileNet-v3 [21], (3) MNASNet [48], and (4) ShuffleNet [37], with 5.3M, 2.2M, 2.5M, and 1.4M number of parameters respectively. For human-activity recognition datasets, we borrow the ConvNet architecture proposed in [9]. All these models consist of an encoder made of multi-layer CNNs followed by a classifier.

FL Settings. We use Flower [6], a customizable open-source FL framework (Python v3.7, Ray v1.11, and Torch v1.12). We run all simulations on a server with 80 Intel Xeon(R) E5-2698 CPUs, 8 Tesla V100 GPUs (16GB), and 504GB system RAM. For all simulations, we use 100 communication rounds, where at each round, UCDs and APs successively train the model. Unless specified otherwise, we consider 100 clients (each having one AP and one UCD). We randomly sample 10% of the clients for training in each round in our initial experiments and later show that our results hold when the client participation ratio is gradually increased to 100%. Data (D) are partitioned using Latent Dirichlet Allocation (LDA) [5, 8]

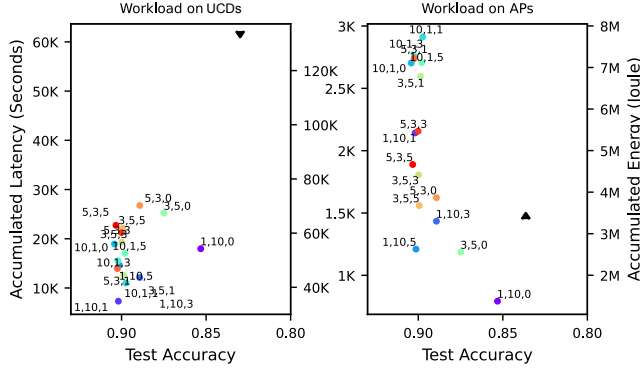


Figure 4: Test accuracy when using different values for parameters α , β , γ in data selection. The \blacktriangledown point in the left figure is the UCD training, and the \blacktriangle point in the right figure is the AP training. It is found that with data selection, Centaur can always achieve higher accuracy than both UCD training and AP training.

without resampling (LDA-Alpha=1000). We refer to prior research [8] about details of LDA’s generative process. After such partition, each client owns $|D|/100$ local samples.

For each client, we randomly select half of the samples and use them for local training of the model. For both APs and UCDs, we consider by default the number of epochs to be 3 with a batch size of 64. The other half of the samples are available with more offline time to simulate the further collection of extra data. APs and UCDs also train more epochs on the extra data while offline. In this setup, we define every unit offline time contributing to one more epoch of training on 20% of these extra local samples. For Equation (2) and (3) in data selection we set α, β, γ as 5, 3, 0, respectively. Figure 4 gives the test accuracy when we set different values for the α, β , and γ in the data selection scheme.

Baselines. (1) AP Training. We consider UCDs as data collection apparatuses only and therefore, UCDs upload collected and stored data samples to their connected APs, so that the training only happens on APs. In this case, the complete model (both the encoder and classifier) is updated because APs in general are considered to have sufficient resources. **(2) UCD Training.** UCDs do not upload the collected data samples. Instead, they conduct training on the data locally. However, as UCDs are typically resource-constrained, only the classifier is considered to be trained on-device. This means that the encoder part is considered to be frozen in this setting.

Mobility Model. In our case, the idea of the mobility model signifies how the mobility patterns of the UCDs (or users) impact the connectivity of the UCD to its AP and eventually to the internet. We define an exclusive Online Association Matrix Ω , which is a binary matrix representing the

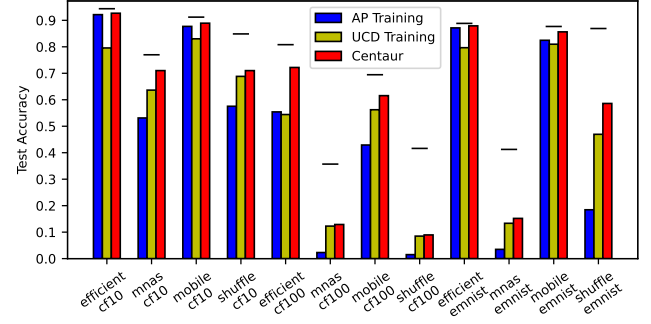


Figure 5: Accuracy of the best classifier for four different encoders, trained on CIFAR10, CIFAR100, and EMNIST. Dash lines (—) above depict the upper-bound accuracy when UCD devices have no resource and connectivity constraints.

user’s exclusive location at a given time instance. Mathematically, Ω is a binary matrix $\mathcal{T} \times \mathcal{S}$ where \mathcal{T} and \mathcal{S} represent the temporal and spatial granularity of Ω matrix, respectively. For example, the rows may represent the time zones of the day (early morning, morning, afternoon, evening, and late night), during which the user moves between three locations like home, office, and a public park, represented by the columns of Ω . Furthermore, we ensure that each row’s sum equals unity, which means the user is present exclusively at a unique location in a given temporal instance. Finally, to simulate the connectivity patterns, we define a connectivity matrix λ , a single row-vector of dimension \mathcal{S} , denoting the connectivity probability across different locations. More specifically, for evaluating Centaur during mobility, we generate the global connectivity matrix λ and the generate matrix Ω , both chosen uniformly at random, for each user to simulate the mobility scenario.

6 Evaluation Results

We present the results when running Centaur compared to conventional FL training methods and compare the approaches using different metrics. We also analyze the impact of data/participation heterogeneity and spatiotemporal coverage on training methods.

6.1 Metrics

In addition to the accuracy of the trained global model on a held-out test set we evaluate the performance of our FL framework, compared to other FL alternatives, using the following metrics.

1) Accuracy. This is the classification accuracy of the trained model on a test set hosted by the central server. For a model obtained at the end of each training round, the test

accuracy is computed as

$$acc \equiv \frac{1}{T} \sum_{i=1}^T \mathbb{1}(\text{argmax}(f_E \circ f_C(\mathbf{X}_i)) = \mathbf{y}_i),$$

where test set has T pairs of $(\mathbf{X}_i, \mathbf{y}_i)$ and $\mathbb{1}(C)$ denote the indicator function that outputs 1 if condition C holds.

2) Multiply–Accumulate (MAC). This operation is a common step that computes the product of two numbers and adds that product to an accumulator ($a \leftarrow a + (b \times c)$); a fundamental operation for both any DNN layers during training and inference. We use `fvcore` [17] library to compute the number of MAC operations. Since `fvcore` only supports counting MACs in a forward pass, and to count MACs in a backward pass, we use the heuristic that FLOPs (*i.e.*, double MACs) ratio of the backward-forward pass is typically between $1\times$ and $3\times$ and most often is $2\times$ based on models' specific layer types, according to previous observations [39].

3) Bandwidth. As the model size (*i.e.*, the encoder or the classifier) can be different in each FL round, we use `fvcore` to count the number of parameters that are communicated in each round. Based on the model size and number of communications among UCDs, APs, and the server, we compute the amount of bandwidth that is consumed. Also, we count the number of sample points that are uploaded from UCDs to APs.

4) Latency. The latency usually has a linear relation with MAC operations, due to the lack of specialized accelerators [32, 33]. Thus, we estimate the latency of model training based on the processor's frequency as - Latency = $c * \frac{\text{Total MACs}}{\text{Processor Frequency}}$. The ratio between MAC operations and the processor's instructions, c , is typically between 1 and 2 based on specific instruction sets/compilers. For simplicity, we assume that each MAC operation translates to two instructions in an MCU (*i.e.*, $c = 2$). Notice that existing processors (*e.g.*, Intel's Load Effective Address) complete one MAC in one instruction [54]), and this only scales the experimental results and does not change the conclusions. Finally, communication latency is estimated based on the total amount of data needed to be transmitted, divided by the up-link speed or the down-link speed of devices.

5) Energy. This is the total execution time multiplied by the processor's consumed power per unit time. The energy consumption of communication can also be calculated based on the total time of transmitting data multiplied by the transmitters' power per unit time. We set the values for UCDs and APs in our simulations as follows. We assume a typical AP to have a CPU frequency of 2GHz, storage capacity of 4GB, power capacity of 1.5mW/MHz with an uplink speed of 10Mbit/s, downlink speed 100Mbit/s, and communication energy of 10W. For a typical UCDs, we assume a CPU frequency of 100MHz, storage capacity of 5MB, power capacity

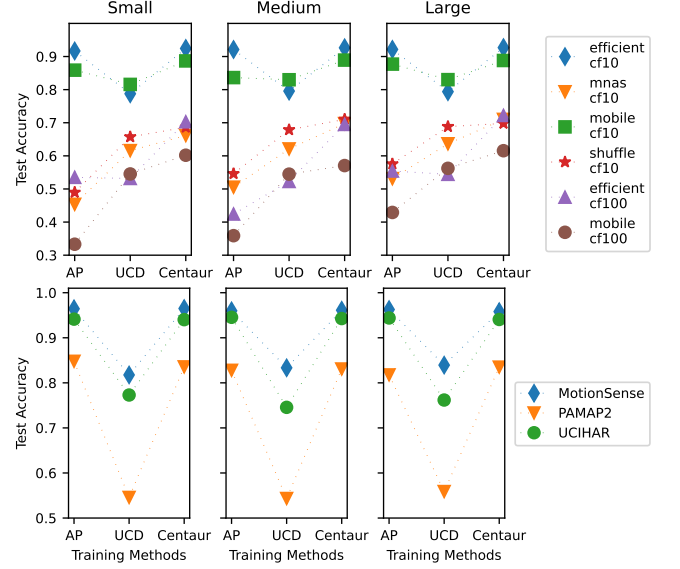


Figure 6: Centaur performance vs. other baselines for different sizes of classifiers: small, medium, and large. (Top) image classification, and (bottom) HAR datasets.

of 0.05mW/MHz with an uplink speed of 2Mbit/s, downlink speed of 2Mbit/s, and communication energy of 0.0001W.

6.2 Model Accuracy

We use the CNN backbone of the four benchmark models described in §5 as the encoders. We examine three classifiers: *small* that is only one fully connected (FC) layer of size z (number of classes), *medium* that has two FC layers of size 64 and z , and *large* that has two FC layers of size 128 and z .

We permute the four encoders and three classifiers and report the test accuracy of Centaur compared to the two other baselines: AP training and UCD training. In Figure 5 we report the highest test accuracy for each encoder across all three classifiers for three datasets. Results show that Centaur outperforms AP training by 0.53% ~ 40.15% and UCD training by 0.45% ~ 17.78%, depending on the settings. There are several settings in which all FL training methods cannot reach a good accuracy, *e.g.*, NASNet and ShuffleNet on CIFAR100, probably because of their relatively small model sizes compared to data complexity. Among them, Centaur still achieves better performance.

In Figure 6 we present the accuracy of different classifiers for each encoder. In the top plot, the results of training on CIFAR10 and CIFAR100 with an accuracy higher than 30% are presented for better visibility. In the bottom plot, we report the results of UCIHAR, MotionSense, and PAMAP2. The results show that Centaur outperforms both UCD training in all classifiers' sizes. The test accuracy also tends to be similar

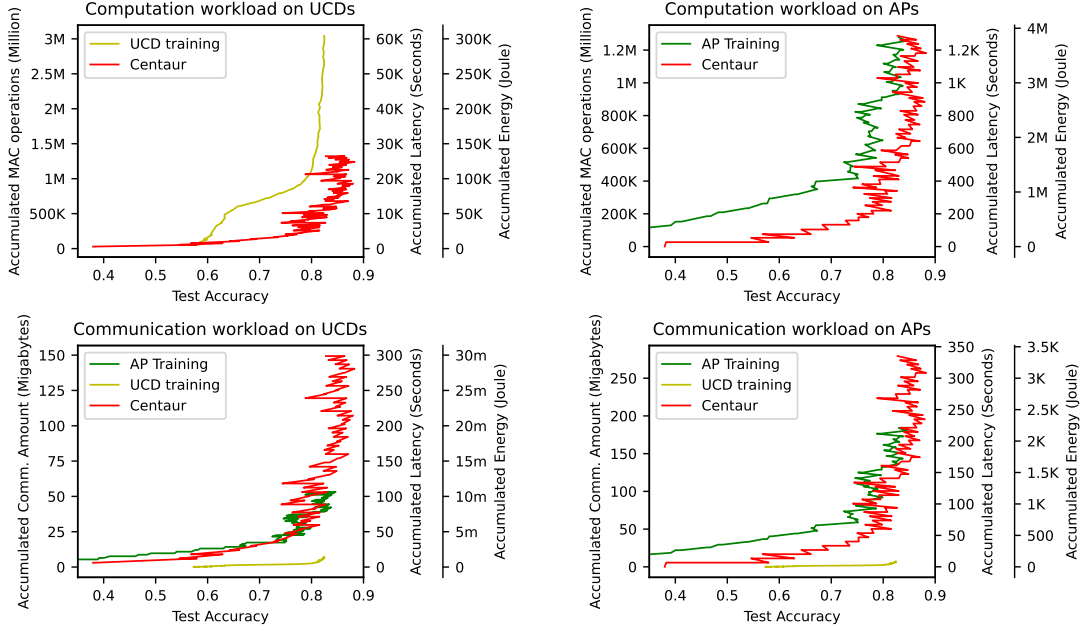


Figure 7: Computation workload of model training on usage-constrained devices (Top Left) and access points (Top Right), and Communication workload of model/data sharing of usage-constrained devices (Bottom Left) and access points (Bottom Right) when achieving specific test accuracy, reported on MobileNetv3 and CIFAR10.

across small, medium, and large classifiers. In addition, the classifier’s sizes may have less impact on more sophisticated encoders (e.g., EfficientNet and MobileNet), which is also observed in a previous work [41]. This may be because an appropriate encoder already produces high-quality features for unseen data that are easy to learn (e.g., CIFAR10), and in such a case, classifier sizes do not make any difference in test accuracy. Similar patterns are observed in HAR datasets. Notice that for HAR datasets, there is currently a lack of publicly accessible pre-trained encoders to start FL with. As a result, we can observe a more significant performance gap compared to image classification, particularly for more complex datasets, e.g., PAMAP2. This lack of pre-trained encoders can also be the reason that, in HAR datasets, the performance of Centaur and AP are almost the same.

6.3 Efficiency

Cost-Accuracy Trade-off. We use CIFAR10, and fix MobileNet-v3 as the encoder and medium size for the classifier. We compute the test accuracy for a range of MAC, Bandwidth, Latency, and Energy budgets. The average size of each sample of CIFAR10 is 30KB. As shown in Figure 7 (top), on both UCD and AP and for all ranges of accuracy, Centaur achieves lower MAC and Latency than both UCD training and AP training. In addition, Figure 7 (bottom) shows that communication Bandwidth and Latency of Centaur is almost the same as

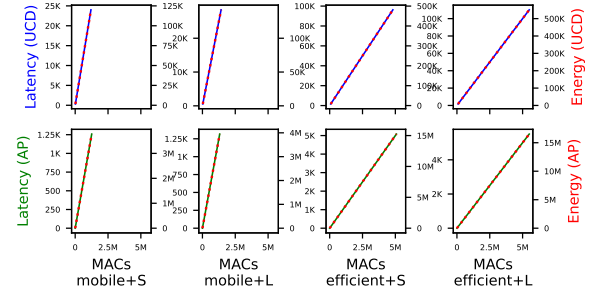


Figure 8: Cost linkage analysis among MAC operations, latency, and energy consumption.

AP training; however, Centaur can achieve a higher test accuracy along with more training steps while consuming more resources. Centaur causes much more communication cost than UCD training, because the training only involves the transmission of the classifier, which is much lighter than the encoder and data samples transmitted by Centaur. However, the accuracy of UCD training cannot go further than 83.10%, while Centaur can reach up to 89.90% accuracy. We remark that model training consumes much more energy and causes much more latency than communication.

Correlation among Cost Metrics. To show the connection between cost metrics, we plot MAC, Latency, and Energy in Figure 8. We observe that both Latency and Energy have

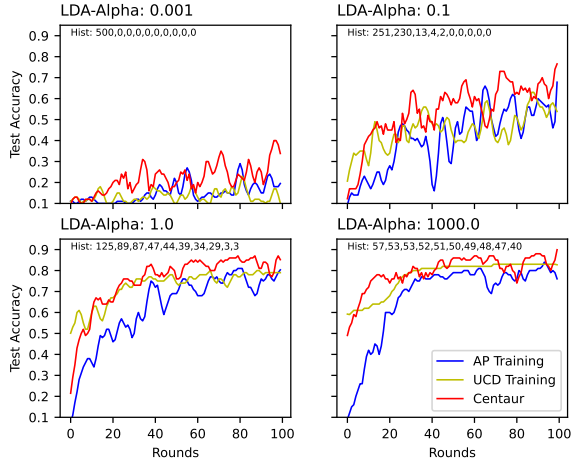


Figure 9: The impacts of imbalanced data partitioning on test accuracy of AP training, UCD training, and Centaur, on MobileNetv3 with CIFAR10 (annotated texts are examples of the classes present on a UCD)

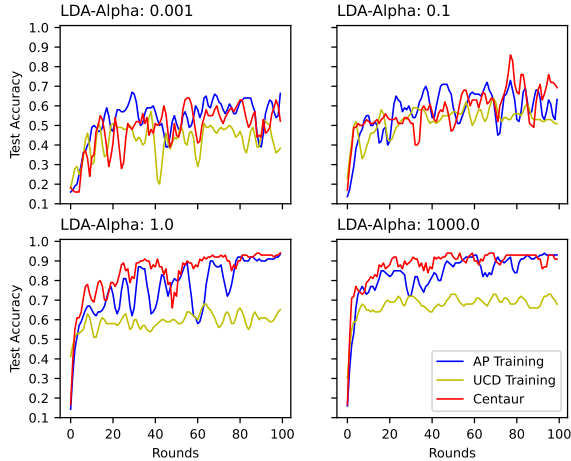


Figure 10: The impacts of imbalanced data partitioning on test accuracy of AP training, UCD training, and Centaur, on ConvNet and UCIHAR dataset dataset.

linear relationships with MAC. Besides, Latency is also linearly correlated with Energy, in such a way that these two entirely overlap when we appropriately scale the y-axes. We remark that Bandwidth also has a similar correlation. Such linear relationships are because of the assumption we made when computing Latency and Energy; however, the actual cost and the relationship among these metrics might not deviate much in practice. Based on such correlations, we can add Latency (or Energy) of model training as well as the communication Bandwidth to get the overall workload. The results shown in Figure 1 indicate that the workload still follows a similar pattern as the computation in model training,

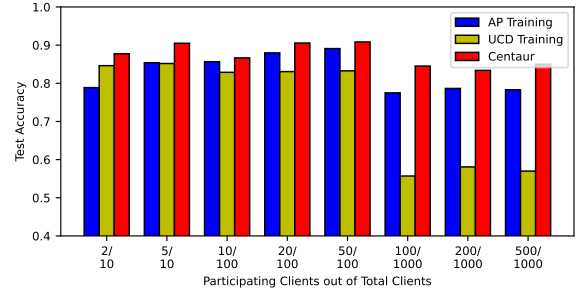


Figure 11: The impact of participating vs. total clients on test accuracy for MobileNetv3 with CIFAR10.

because the training workload significantly overweight the communication workload.

6.4 Data and Participation Heterogeneity

Centaur is robust to data heterogeneity. To create imbalanced non-IID data partitions among clients, we use LDA as defined in § 6.1. Next, we set different values for LDA-Alpha to manipulate the levels of non-IID data partitions. Figure 9 and Figure 10 show the results when LDA-Alpha are changing from 0.001, to 0.1, to 1, and to 1000. The smaller LDA-Alpha is, the less balanced the dataset is. We also annotate some examples of class distribution in Figure 9, demonstrating that LDA-Alpha= 0.001 generates almost 1 class per client, while LDA-Alpha= 1000 generates almost uniform classes per client. Results show that in all cases Centaur can reach higher test accuracy than both AP and UCD training. We remark that due to the retraining of the encoder, both Centaur and AP training can cause more fluctuations than UCD training; this is especially obvious when data distribution tends to be IID (e.g., when LDA-Alpha= 1000 in Figure 9).

Centauro scales well with higher total and participating clients. We further scale the FL training problem with the number of total clients from 10 to 1000. 10%, 20%, and 50% of them are selected respectively as participating clients in each round. Figure 11 shows Centauro achieves higher test accuracy compared to both UCD training and AP training. Specifically, with a higher participation rate, all training methods tend to have better performance. However, with a much larger number of total clients (e.g., 1000), the test accuracy is reduced, because the same size of data is partitioned into more portions. Also, with such more fragmented data partitioning, Centauro has much accuracy gain when compared to UCD training.

6.5 Performance of Centaur under Mobility

We evaluate situations when the connection probability λ changes based on the mobility model defined in §6.1. For a

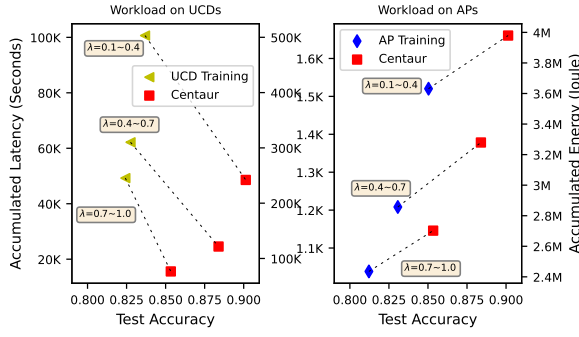


Figure 12: The performance of access point (AP) training, usage-constrained device (UCD) training, and partition-based federated learning (Centaur) under different connection probabilities λ , reported on MobileNetV3 and CIFAR10.

more readable visualization, we bucket λ in three different ranges of $\lambda \in [0.1, 0.4]$, $\lambda \in [0.4, 0.7]$, and $\lambda \in [0.7, 1.0]$ and report the corresponding Accuracy of Centaur when the UCDs are mobile. Results reported in Figure 12 show that Centaur always has higher efficiency than standard UCD training while incurring a higher latency than direct AP training. Specifically, regarding the much important UCD side, Centaur gains 6.45%, 5.64%, and 4.11% higher accuracy with 51.73%, 60.48%, and 68.35% lower cost both in terms of energy and latency across the different ranges of λ . Interestingly, we also observe a rise in accuracy with lower connectivity probability. The primary reason is attributed to the overall design of our experimental setup, whereby we make a realistic assumption that with limited connectivity, these UCDs can gather more data and perform the data selection. Additionally, with this selected data, the device trains the classifier for an extended number of epochs, thus boosting its accuracy.

7 Conclusions

We propose an efficient training method that leverages data selection to improve learning and reduce computational costs in multidevice federated learning. Our approach allows partition-based training and aggregation on resource-constrained devices, supported by resourceful companion devices. Our evaluations over various scenarios confirm that our proposed solution improves model accuracy while reducing system overhead.

Limitations. We use standard FedAvg in our implementation, but Centaur can accommodate other FL aggregation strategies. Layer-wise FL methods that perform model training in a partitioned manner, such as FedMA [52], can also be integrated. We evaluated Centaur on supervised tasks, but

a complementary approach can be suggested for semi- or unsupervised tasks. Finally, the gradient-based data selection is a heuristic approach that can be susceptible to outliers and out-of-distribution data, thus one can expand Centaur to resolve these concerns.

References

- [1] Mehdi Salehi Heydar Abad, Emre Ozfatura, Deniz Gunduz, and Ozgur Ercetin. [n. d.]. Hierarchical federated learning across heterogeneous cellular networks. In *ICASSP*.
- [2] Alaa Awad Abdellatif, Naram Mhaisen, Amr Mohamed, Aiman Erbad, Mohsen Guizani, Zaher Dawy, and Wassim Nasreddine. 2022. Communication-efficient hierarchical federated learning for IoT heterogeneous systems with imbalanced data. *Future Generation Computer Systems* (2022).
- [3] D. Anguita, Alessandro Ghio, L. Oneto, Xavier Parra, and Jorge Luis Reyes-Ortiz. 2013. A Public Domain Dataset for Human Activity Recognition using Smartphones. In *ESANN*.
- [4] Colby Banbury, Chuteng Zhou, Igor Fedorov, Ramon Matas, Urmish Thakker, Dibakar Gope, Vijay Janapa Reddi, Matthew Mattina, and Paul Whatmough. 2021. Micronets: Neural network architectures for deploying tinyml applications on commodity microcontrollers. *MLSys* (2021).
- [5] Daniel J Beutel, Taner Topal, Akhil Mathur, Xinchu Qiu, Javier Fernandez-Marques, Yan Gao, Lorenzo Sani, Kwing Hei Li, Titouan Parcollet, Pedro Porto Buarque de Gusmão, et al. 2022. Flower: A friendly federated learning framework. (2022).
- [6] Daniel J Beutel, Taner Topal, Akhil Mathur, Xinchu Qiu, Titouan Parcollet, and Nicholas D Lane. 2020. Flower: A Friendly Federated Learning Research Framework. (2020).
- [7] Sameer Bibikar, Haris Vikalo, Zhangyang Wang, and Xiaohan Chen. 2022. Federated dynamic sparse training: Computing less, communicating less, yet learning better. In *AAAI*.
- [8] David M Blei, Andrew Y Ng, and Michael I Jordan. 2003. Latent dirichlet allocation. *JMLR* (2003).
- [9] Youngjae Chang, Akhil Mathur, Anton Isopoussu, Junehwa Song, and Fahim Kawsar. 2020. A systematic study of unsupervised domain adaptation for robust human-activity recognition. *IMWUT* (2020).
- [10] Hyunsung Cho, Akhil Mathur, and Fahim Kawsar. 2022. Flame: Federated learning across multi-device environments. *IMWUT* (2022).
- [11] Gregory Cohen, Saeed Afshar, Jonathan Tapon, and Andre Van Schaik. 2017. EMNIST: Extending MNIST to handwritten letters. In *IJCNN*.
- [12] Rong Dai, Li Shen, Fengxiang He, Xinmei Tian, and Dacheng Tao. 2022. DisPFL: Towards Communication-Efficient Personalized Federated Learning via Decentralized Sparse Training. (2022).
- [13] Robert David, Jared Duke, Advait Jain, Vijay Janapa Reddi, Nat Jeffries, Jian Li, Nick Kreeger, Ian Nappier, Meghna Natraj, Tiezheng Wang, et al. 2021. Tensorflow lite micro: Embedded machine learning for tinyml systems. *MLSys* (2021).
- [14] Jia Deng, Wei Dong, Richard Socher, Li-Jia Li, Kai Li, and Li Fei-Fei. 2009. Imagenet: A large-scale hierarchical image database. In *CVPR*.
- [15] Enmao Diao, Jie Ding, and Vahid Tarokh. 2020. HeteroFL: Computation and communication efficient federated learning for heterogeneous clients. (2020).
- [16] Fotios Drakopoulos, Deepak Baby, and Sarah Verhulst. 2019. Real-time audio processing on a Raspberry Pi using deep neural networks. In *23rd International Congress on Acoustics*.
- [17] FAIR. 2019. fvcare.

- [18] Igor Fedorov, Ryan P Adams, Matthew Mattina, and Paul Whatmough. 2019. Sparse: Sparse architecture search for cnns on resource-constrained microcontrollers. *NeurIPS* (2019).
- [19] Otkrist Gupta and Ramesh Raskar. 2018. Distributed learning of deep neural network over multiple agents. *Network and Computer Applications* (2018).
- [20] Andrew Hard, Kanishka Rao, Rajiv Mathews, Swaroop Ramaswamy, Françoise Beaufays, Sean Augenstein, Hubert Eichner, Chloé Kiddon, and Daniel Ramage. 2018. Federated learning for mobile keyboard prediction. (2018).
- [21] Andrew Howard, Mark Sandler, Grace Chu, Liang-Chieh Chen, Bo Chen, Mingxing Tan, Weijun Wang, Yukun Zhu, Ruoming Pang, Vijay Vasudevan, et al. 2019. Searching for mobilenetv3. In *CVPR*.
- [22] Bashima Islam and Shahriar Nirjon. 2019. Zygard: Time-sensitive on-device deep inference and adaptation on intermittently-powered systems. (2019).
- [23] Angela H Jiang, Daniel L-K Wong, Giulio Zhou, David G Andersen, Jeffrey Dean, Gregory R Ganger, Gauri Joshi, Michael Kaminsky, Michael Kozuch, Zachary C Lipton, et al. 2019. Accelerating deep learning by focusing on the biggest losers. (2019).
- [24] Peter Kairouz, H. Brendan McMahan, and et al. 2021. Advances and Open Problems in Federated Learning. *Foundations and Trends® in ML* (2021).
- [25] Honggu Kang, Seohyeon Cha, Jinwoo Shin, Jongmyeong Lee, and Joonhyuk Kang. 2023. NeFL: Nested Federated Learning for Heterogeneous Clients. (2023).
- [26] Angelos Katharopoulos and François Fleuret. 2018. Not all samples are created equal: Deep learning with importance sampling. In *ICML*.
- [27] Kavya Koppurapu, Eric Lin, John G Breslin, and Bharath Sudharsan. 2022. TinyFedTL: Federated Transfer Learning on Ubiquitous Tiny IoT Devices. In *PerCom Workshops*.
- [28] Alex Krizhevsky, Geoffrey Hinton, et al. 2009. Learning multiple layers of features from tiny images. (2009).
- [29] Fan Lai, Xiangfeng Zhu, Harsha V. Madhyastha, and Mosharaf Chowdhury. 2021. Oort: Efficient Federated Learning via Guided Participant Selection. In *OSDI*.
- [30] Seulki Lee, Bashima Islam, Yubo Luo, and Shahriar Nirjon. 2019. Intermittent learning: On-device machine learning on intermittently powered system. *IMWUT* (2019).
- [31] Ang Li, Jingwei Sun, Pengcheng Li, Yu Pu, Hai Li, and Yiran Chen. 2021. Hermes: an efficient federated learning framework for heterogeneous mobile clients. In *MobiCom*.
- [32] Edgar Liberis, Łukasz Dudziak, and Nicholas D Lane. 2021. μ NAS: Constrained Neural Architecture Search for Microcontrollers.
- [33] Ji Lin, Ligeng Zhu, Wei-Ming Chen, Wei-Chen Wang, Chuang Gan, and Song Han. 2022. On-device training under 256kb memory. *NeurIPS* (2022).
- [34] Tao Lin, Lingjing Kong, Sebastian U Stich, and Martin Jaggi. 2020. Ensemble distillation for robust model fusion in federated learning. *NeurIPS* (2020).
- [35] Lumin Liu, Jun Zhang, SH Song, and Khaled B Letaief. 2020. Client-edge-cloud hierarchical federated learning. In *IEEE ICC*.
- [36] Wang Lu and Jindong Wang. 2023. PersonalizedFL: Personalized Federated Learning Toolkit. <https://github.com/microsoft/PersonalizedFL>.
- [37] Ningning Ma, Xiangyu Zhang, Hai-Tao Zheng, and Jian Sun. 2018. Shufflenet v2: Practical guidelines for efficient cnn architecture design. In *ECCV*.
- [38] Mohammad Malekzadeh, Richard G Clegg, Andrea Cavallaro, and Hamed Haddadi. 2019. Mobile sensor data anonymization. In *IoTDL*. 49–58.
- [39] Jsewillamol Marius Hobbhahn. 2021. *What's the backward-forward FLOP ratio for Neural Networks?*
- [40] H.Brendan McMahan, Eider Moore, Daniel Ramage, Seth Hampson, and Blaise Agüera y Arcas. 2017. Communication-Efficient Learning of Deep Networks from Decentralized Data. In *AISTATS*.
- [41] Fan Mo, Hamed Haddadi, Kleomenis Katevas, Eduard Marin, Diego Perino, and Nicolas Kourtellis. 2021. PPFL: privacy-preserving federated learning with trusted execution environments. In *MobiSys*.
- [42] Fan Mo and Jia Zhou. 2021. Adapting smartwatch interfaces to hand gestures during movements: offset models and the C-shaped pattern of tapping. *Journal of Ambient Intelligence and Humanized Computing* (2021).
- [43] Chaoyue Niu, Fan Wu, Shaojie Tang, Lifeng Hua, Rongfei Jia, Chengfei Lv, Zhihua Wu, and Guihai Chen. 2020. Billion-scale federated learning on mobile clients: A submodel design with tunable privacy. In *MobiCom*.
- [44] Franz Papst, Katharina Schodl, and Olga Saukh. [n. d.]. Exploring co-dependency of iot data quality and model robustness in precision cattle farming. In *SenSys*.
- [45] Jong-Ik Park and Carlee Joe-Wong. 2024. Federated Learning with Flexible Architectures. In *ECML PKDD*.
- [46] Attila Reiss and Didier Stricker. 2012. Introducing a new benchmarked dataset for activity monitoring. In *ISWC*.
- [47] Suranga Seneviratne, Yining Hu, Tham Nguyen, Guohao Lan, Sara Khalifa, Kanchana Thilakarathna, Mahbub Hassan, and Aruna Seneviratne. 2017. A survey of wearable devices and challenges. *IEEE Communications Surveys & Tutorials* (2017).
- [48] Mingxing Tan, Bo Chen, Ruoming Pang, Vijay Vasudevan, Mark Sandler, Andrew Howard, and Quoc V Le. 2019. Mnasnet: Platform-aware neural architecture search for mobile. In *CVPR*.
- [49] Mingxing Tan and Quoc Le. 2021. Efficientnetv2: Smaller models and faster training. In *ICML*.
- [50] Chandra Thapa, Pathum Chamikara Mahawaga Arachchige, Seyit Camtepe, and Lichao Sun. 2022. Splitfed: When federated learning meets split learning. In *AAAI*.
- [51] Delia Velasco-Montero, Jorge Fernández-Berni, Ricardo Carmona-Galán, and Ángel Rodríguez-Vázquez. 2018. Performance analysis of real-time DNN inference on Raspberry Pi. In *Real-Time Image and Video Processing*.
- [52] Hongyi Wang, Mikhail Yurochkin, Yuekai Sun, Dimitris Papailiopoulos, and Yasaman Khazaeni. 2020. Federated learning with matched averaging. (2020).
- [53] Karl Weiss, Taghi M Khoshgoftaar, and DingDing Wang. 2016. A survey of transfer learning. *Journal of Big data* (2016).
- [54] WikiBooks. 2021. x86 Assembly/Data Transfer.
- [55] Kunran Xu, Yishi Li, Huawei Zhang, Rui Lai, and Lin Gu. 2022. EtinyNet: Extremely Tiny Network for TinyML. (2022).
- [56] Qian Yang, Jianyi Zhang, Weituo Hao, Gregory P Spell, and Lawrence Carin. 2021. Flop: Federated learning on medical datasets using partial networks. In *KDD*.
- [57] Jie Zhang, Song Guo, Xiaosong Ma, Haozhao Wang, Wenchao Xu, and Feijie Wu. 2021. Parameterized knowledge transfer for personalized federated learning. *NeurIPS* (2021).
- [58] Lan Zhang, Dapeng Wu, and Xiaoyong Yuan. 2021. FedZKT: Zero-Shot Knowledge Transfer towards Resource-Constrained Federated Learning with Heterogeneous On-Device Models. (2021).
- [59] Tuo Zhang, Lei Gao, Chaoyang He, Mi Zhang, Bhaskar Krishnamachari, and A Salman Avestimehr. 2022. Federated learning for the internet of things: Applications, challenges, and opportunities. *IEEE Internet of Things Magazine* (2022).